Multi-Stage FE Simulation of Hot Ring Rolling

C. Wang[a] and H. J. M. Geijselaers[b] and A. H. van den Boogaard[b]

[a]*Materials innovation institute (M2i), Delft, the Netherlands*
[b]*University of Twente, Section of Applied Mechanics, Enschede, the Netherlands*

Abstract. As a unique and important member of the metal forming family, ring rolling provides a cost effective process route to manufacture seamless rings. Applications of ring rolling cover a wide range of products in aerospace, automotive and civil engineering industries [1]. Above the recrystallization temperature of the material, hot ring rolling begins with the upsetting of the billet cut from raw stock. Next a punch pierces the hot upset billet to form a hole through the billet. This billet, referred to as preform, is then rolled by the ring rolling mill. For an accurate simulation of hot ring rolling, it is crucial to include the deformations, stresses and strains from the upsetting and piercing process as initial conditions for the rolling stage. In this work, multi-stage FE simulations of hot ring rolling process were performed by mapping the local deformation state of the workpiece from one step to the next one. The simulations of upsetting and piercing stages were carried out by 2D axisymmetric models using adaptive remeshing and element erosion. The workpiece for the ring rolling stage was subsequently obtained after performing a 2D to 3D mapping. The commercial FE package LS-DYNA was used for the study and user defined subroutines were implemented to complete the control algorithm. The simulation results were analyzed and also compared with those from the single-stage FE model of hot ring rolling.

Keywords: Hot ring rolling, Preform, Multi-stage FE simulations, Mapping.
PACS: 81.20.Wk

INTRODUCTION

Ring rolling is an advanced metal forming process to produce seamless rings with different sizes and profiles. A hot ring rolling process begins with forging a preform, which is a piece of hot upset metal with a complete hole in the middle. Figure 1(a) shows a preform forging process in the industrial production of a bearing race. The forged thick billet is then rolled into a thin ring in the ring rolling mill. A radial axial ring rolling machine is depicted diagrammatically in figure 1(b) using the finite element model setup in this paper. Typically two rolling processes are done simultaneously, radial rolling and axial rolling. In the radial stage, the ring thickness is gradually reduced, while the axial stage serves to control the final width of the ring. Both processes involve small local deformation increments which are applied many times (typically between 10 and 100). During the rolling, the ring material experiences a very complex deformation history.

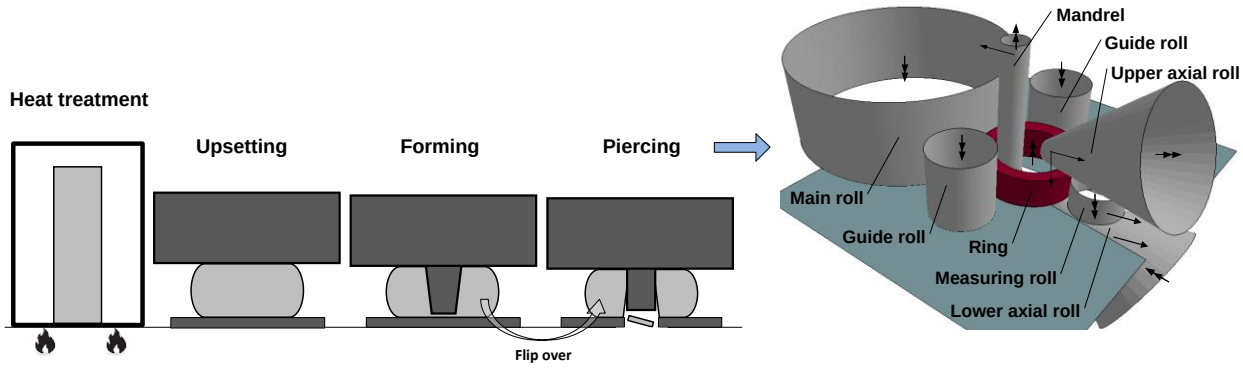

FIGURE 1. Process chain of hot ring rolling: (a) preform forging and (b) ring rolling.

The ring rolling process has been subject to a number of experimental and numerical studies reviewed in [1]. Recently more studies focused on the advanced numerical simulation of radial axial ring rolling (RARR) process by

finite element analysis (FEA). Wang et al. [2] coupled a user program in FE model to control the movements of the guide and axial rolls. Yeom et al. [3] proposed an optimum process condition for large titanium alloy rings by calculation method and FEA. Hua et al. [4] investigated the ring stiffness determined by pressure of guide roll using FE simulation. Zhou et al. [5-6] investigated the effects of roll size and some key process parameters on strain and temperature distributions, respectively, for 42CrMo steel and alloy steel large ring based on coupled thermal mechanical FE models. Zhou et al. [7] studied the forming defects with the help of a FE model with hydraulic adjustment mechanism. Jenkouk et al. [8] simulated the RARR with an integrated industrial control package for a more realistic approach. Giorleo et al. [9] validated FE simulation based on the industrial process. However, Preform forging was not included in these studies. Most of them used an ideal blank, which has a rectangular cross section. The geometry of the initial ring billet with a processing residue in [2] was supplied from the literature. Preform forging is illustrated in [9] but not conducted in the simulation. The deformation history of the preform was not taken into consideration for the RARR simulations. In a very recent study, Qian et al. [10] developed a RARR FE model of combined blank-forging and rolling. The strain and temperature distributions are compared between simulations with ideal ring blank and forged ring blank.

In this work, the multi-stage simulations of hot ring rolling of 100CrMnMoSi8-4-6 bearing steel including preform forging are presented though an efficient and flexible 2D to 3D procedure. The focus of this paper is to show the differences on stress state and roll force with and without considering the deformation history of the preform, particularly on the early stage of ring rolling by numerical simulations.

FINITE ELEMENT SIMULATION

In order to model the process chain of hot ring rolling, the deformation state of the billet was mapped from one step to the next one. Between every two forging steps, stress relaxation steps were also performed to deliver only the residual stresses to the next step. After having the preform forged in the 2D axisymmetric simulations, a preform with strains and residual stresses was obtained by sweeping the 2D section to 3D solid. Two preforms were simulated from two different forming plans. Next these two preforms as well as a prepared 3D ideal blank without deformation were all ring rolled. The ring rolling model has a user defined control algorithm to stabilize this complex process, especially to handle the difficulties introduced by the irregular shape of the preform. A viscoplastic material model was used in the simulations.

Preform forging

The preform forging simulations followed the procedure as shown in figure 2. The further upsetting by the punch after piercing process, which made the difference between Preform A and Preform B was to flatten the axial surfaces of the preform for the benefit of the rolling stage. All the geometric parameters and process parameters are based on the actual industrial process.

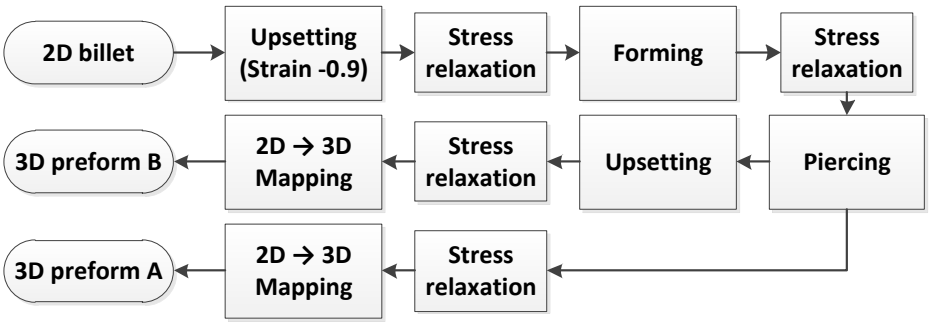

FIGURE 2. The simulation procedure of preform forging.

Upsetting, Forming and Piercing

2D axisymmetric models were built for the upsetting, forming and piercing steps. Adaptive remeshing was applied to avoid over distorted elements for this large deformation case and very fine characteristic element size was

controlled for accurate results. The applied high frequency adaptive remeshing on a 2D model was not expensive on the computational time. The element erosion technique was included in the piercing step to punch out the web of metal left after the forming step. Considering the specimen used in this study, a principal strain based element erosion criterion was applied in the simulations [11]. However, the accurate value of the failure strain requires further comparison with experiment. Figure 3 shows the simulation results of equivalent plastic strain after each step.

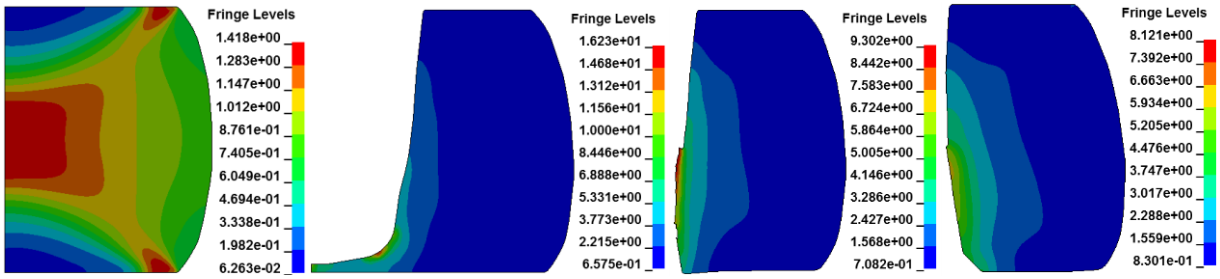

(a) (b) (c) (d)

FIGURE 3. Contour plots of equivalent plastic strain after (a) upsetting; (b) forming; (c) piercing of Preform A; (d) piercing of Preform B.

Stress Relaxation

It is realistic to have a stress relaxation step in the modeling of a multi-stage forming process. To avoid dynamic problems the stress relaxation model used an implicit solver while all the other steps used an explicit solver. It can be found that the hydrostatic tension zone (negative pressure) shifted after the relaxation.

Mapping

After the piercing and the final stress relaxation, adapting a mesh to mesh solution, the two billets were first mapped to a target 2D mesh tailored for the rolling stage. Then they were swept to solid preforms by performing a 2D to 3D mapping. This was done by a FORTRAN code programmed in this study. Figure 4 shows the final preforms from a cross sectional view. It can be observed that the two different piercing procedures resulted in different shapes as well as different strain and stress distributions. Large plastic strain regions are shown in inner sides of the preforms.

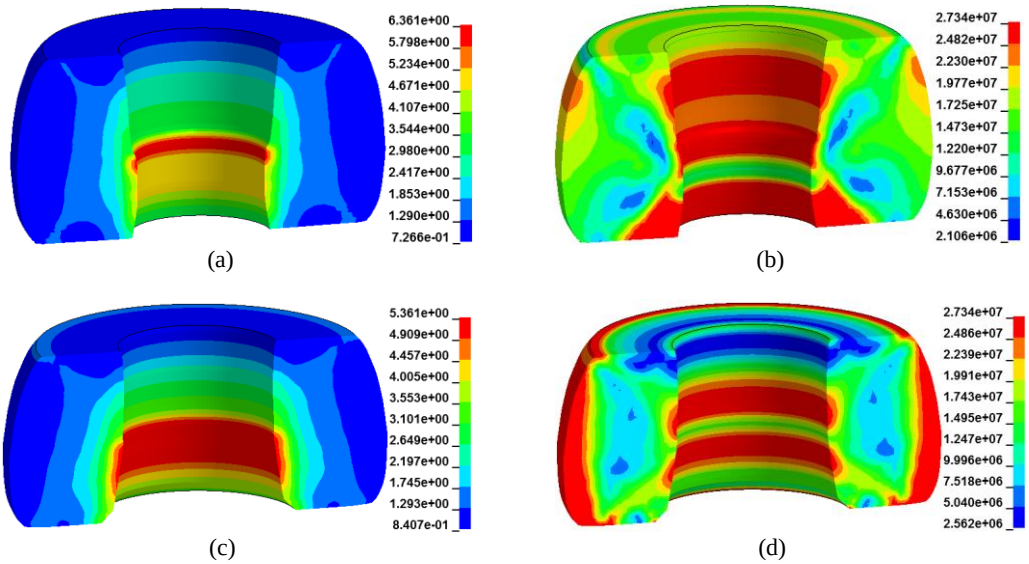

(a) (b) (c) (d)

FIGURE 4. Cross sectional view of two 3D preforms: (a) and (b) contour plots of equivalent plastic strain and von Mises stress of Preform A; (c) and (d) contour plots of equivalent plastic strain and von Mises stress of Preform B.

Ring Rolling

The ring rolling model built in this study is shown in figure 1(b). The complete billet width was modeled, therefore the support plane and gravity force were also taken into consideration. The roll size was also defined based on the industrial ring rolling mill.

In a previous study [12,8], an analytical control algorithm for guide rolls and axial rolls was described and implemented successfully in a finite element model of the ring rolling process using the simulation feedback response. It has also been adapted and implemented in this model to control the motions of rolls. The rotational displacements of guide rolls around fixed hinge, the angular velocities of axial rolls as well as the translational displacements of axial rolls are defined separately as a function of the diameter of the ring workpiece in time. After having the control routine implemented in LS-DYNA, the motion of rolls during the simulation are imposed using the simulation response data, which are the kinematical quantities of the sensor node on the measuring roll. The prescribed process conditions are plotted in Figure 5 and the rotational speed of the main roll was kept constant. Since in this explicit calculation the material undergoes large rotation, 2nd order objective stress updates were used.

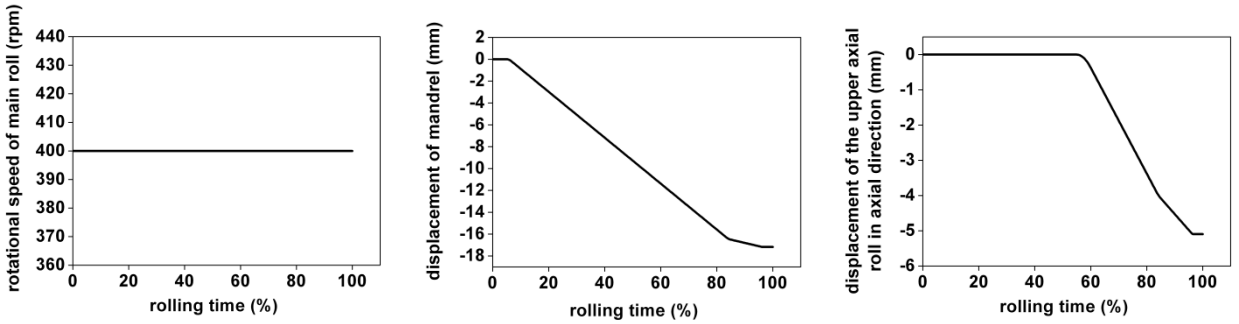

(a) (b) (c)

FIGURE 5. Prescribed process conditions: (a) rotational speed of the main roll; (b) displacement of mandrel in radial direction; (b) displacement of the upper axial roll in axial direction.

RESULTS AND DISCUSSIONS

An ideal blank that has a rectangular cross section was created based on the two preforms. The three initial billets, i.e., two forged preforms and one ideal blank with rectangular cross section were all rolled under the same rolling plan. The differences on deformation state are clearly observed between ideal blank and the two preforms. Figure 6 shows the equivalent plastic strain distribution of the workpiece from different views, during the rolling of Preform A. From Figure 6(b), It can be observed that, the bulge of the preform was getting rolled at initial stage of rolling with a relatively small contact area. With mandrel feeding and constrains at two roll gaps, the material flowed to the corners to form the new rectangular cross section as shown in figure 6(c). The contribution of preform forging to the plastic strain is perceptible even in the final state as shown in figure 6(d).

For the preforms A and B it can be further noticed that there is no ring growth at the beginning. The diameter of the ring was actually decreased due to the phenomenon mentioned above. Naturally the guide rolls, which rotated around the fixed hinge, also moved towards the ring to stabilize the process.

Since porosity increases when hydrostatic pressure becomes more negative (hydrostatic tension) during the forming process, materials are sensitive to hydrostatic tension if there exist micro voids. The two forged preforms have considerable hydrostatic tension zones at the beginning as shown in Figure 7(a) and 7(b). For Preform A it mainly locates in the middle of the inner surface, whereas for the preform B it appears at the outer surface. The history of the minimum hydrostatic pressure in early stage of ring rolling is plotted in Figure 7(c) for ideal blank and preforms. It can be concluded that, over time lower hydrostatic pressure exists in the ring workpiece of the two preforms. Figure 7(d-f) illustrates the hydrostatic pressure distribution in the two deformation zones, i.e., at radial roll gap and axial roll gap, for the three ring workpieces. For ideal blank the distribution of hydrostatic tension is roughly symmetrical along radial direction and axial direction at two roll gaps respectively. It can be seen from Figure 7(e) and 7(f) for Preform A and Preform B that, the distribution of hydrostatic tension is highly influenced by the contact modes associated with their irregular cross section shapes. The high hydrostatic tension zone firstly appears where the ring has no direct contact with the mandrel.

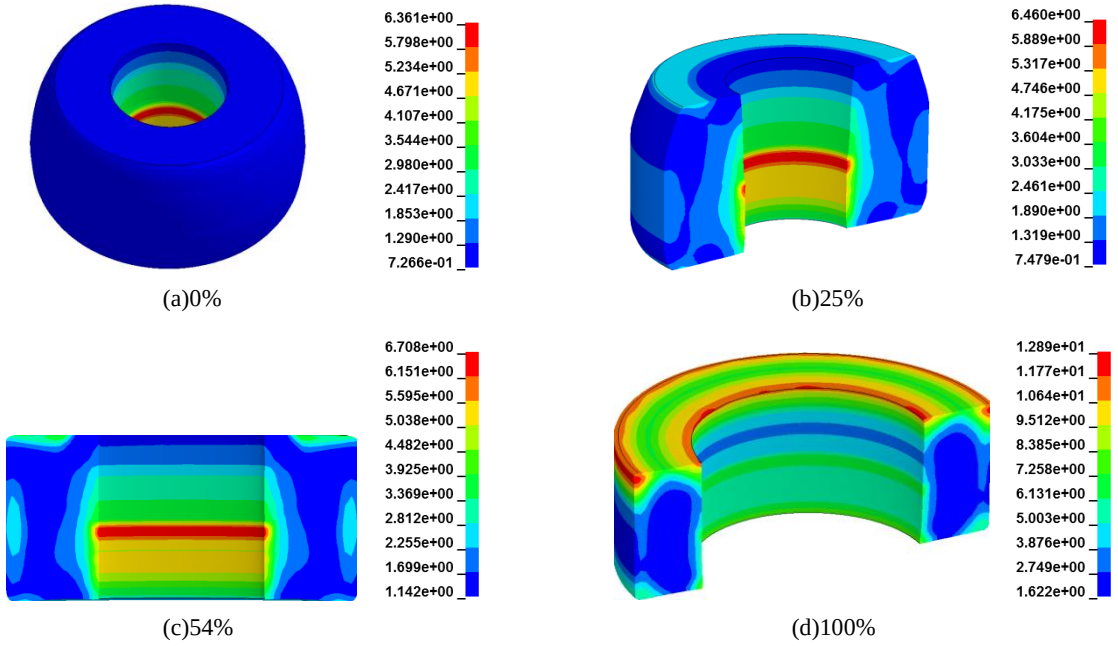

FIGURE 6. Equivalent plastic strain plots of the ring workpiece (Preform A) at different rolling time (%).

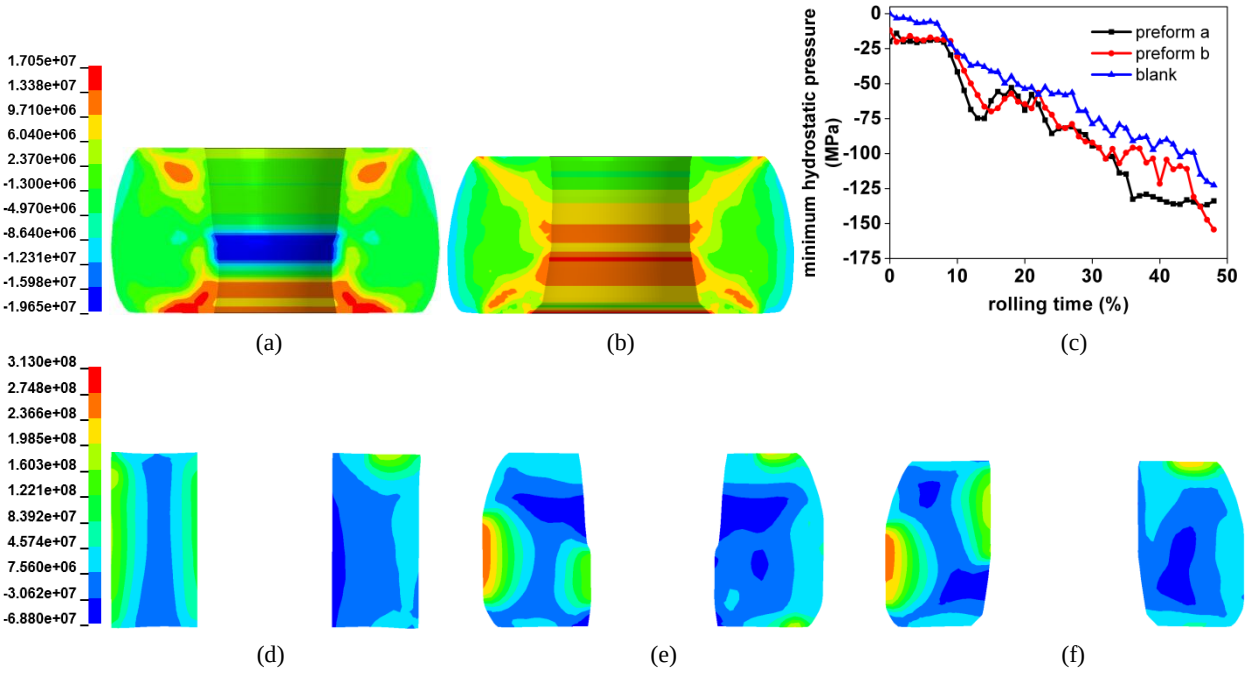

FIGURE 7. Plots of distribution and evolution of hydrostatic pressure: hydrostatic pressure distribution of Preform A before rolling; (b) hydrostatic pressure distribution of Preform B before rolling. (c) minimum hydrostatic pressure over time during early stage of ring rolling. (d-f) hydrostatic pressure distribution at 20% rolling time in the radial roll gap (left) and axial roll gap (right) of ideal blank, Preform A and Preform B respectively.

An investigation on the roll force has been also made. At the radial roll gap between main roll and mandrel, where the geometric irregularity mainly remains on the preforms, the force on the mandrel is overall considerably larger for two preforms than that for the blank as shown in figure 8(a). It is lower at the beginning because of the relatively smaller contact area. From figure 8(b) the roll force at axial roll gap reaches the same conclusion only larger difference between Preform A and Preform B is observed, which is expected from the difference on the axial

surfaces between them. Flat axial surfaces on Preform B results in larger contact area between the billet and the axial roll.

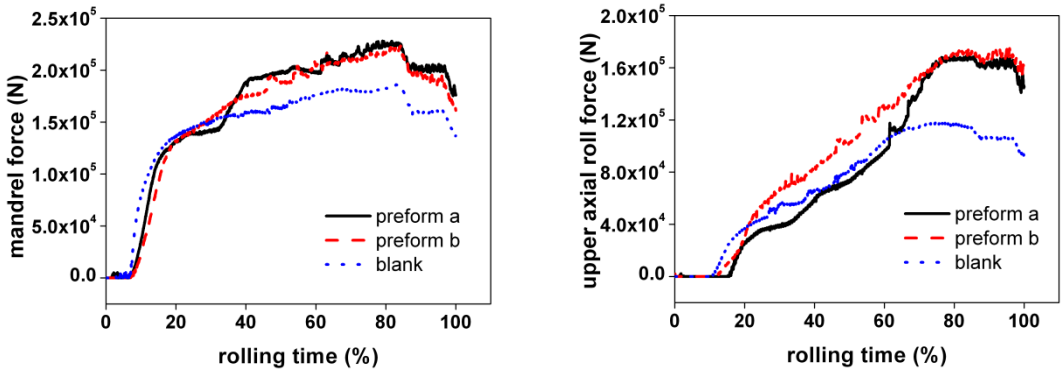

(a) (b)

FIGURE 8. The roll forces at the radial and axial roll gaps over time.

The computational time of the MPP (massively parallel processing) execution of all the simulations for one product spent 25 hours with 12 processors (Intel® Xeon® CPU X5650@2.67GHz).

CONCLUSIONS

Multi-stage finite element simulations to model the hot ring rolling process from the preforming forging to the ring rolling have been done by an efficient 2D to 3D procedure in this study. Many modeling techniques are included for both the computational efficiency and calculation accuracy. The feedback control using simulation response data grants a stable process in the rolling stage simulations. The FE simulation shows the stress state and roll force during ring rolling of ideal blank and forged preforms. It has been observed that higher hydrostatic tension exists in the workpiece during the rolling of forged preforms. The investigation on the simulation results has numerically confirmed the differences with and without considering preform forging. This indicates the significance of the process chain modeling. Further work will focus on the comparison with the experiment.

ACKNOWLEDGMENTS

This research was carried out under project number M41.1.11418 in the framework of the Research Program of the Materials innovation institute M2i (www.m2i.nl). The industrial partner, SKF Group Manufacturing Development Centre is gratefully acknowledged for the contributions to this research.

REFERENCES

1. J. M. Allwood, A. E. Tekkaya and T. F. Stanistreet, *Steel Research International* **76**, 111-120 (2005).
2. Z. W. Wang et al., *Journal of Materials Processing Technology* **182**, 374-381 (2007).
3. J. T. Yeom et al., *Journal of Materials Processing Technology* **187-188**, 747-751 (2007).
4. L. Hua, L. B. Pan and J. Lan, *Journal of Materials Processing Technology* **209**, 2570-2575 (2009).
5. G. Zhou, et al., *Computational Materials Science* **50**, 65-76 (2010).
6. G. Zhou, L. Hua and D.S. Qian, *Computational Materials Science* **50**, 911-924 (2011).
7. J. Zhou, et al., *International Journal of Advanced Manufacturing Technology* **55**, 95-106 (2011).
8. V. Jenkouk, et al., *CIRP Annals Manufacturing Technology* **61**, 267-270 (2012).
9. L. Giorleo, C. Giardini and E. Ceretti, *The international journal of material forming* **6**, 145-152 (2013).
10. D. S. Qian and Y. Pan, *Computational Materials Science* **70**, 24-36 (2013).
11. S. Szyniszewski et al., “Tensile and shear element erosion in metal foams” in *12th International LS-DYNA Users Conference.*
12. C. Wang, "Motion control of the rolling tools in a finite element model of the ring rolling process", Master Thesis, RWTH Aachen University, (2010).